Team BengalSub’s Autonomous Underwater Vehicle: Hangor 2.0

Sudipto Mondal, Md Masrul Khan, Khondokar Radwanur Rahman, Sirajum Munir, Ariyan Siddique, Rahul Debnath, Asadullah Al Galib, An Nafew, Rubaiyat H Rahman, Hasin Israque, Md Tanvir Rahman, Mohammad Sanjeed Rahman, Abeed Mahmood, and Rasel Ahmed

***Abstract*— For RoboSub 2026, Team BengalSub presents (Hangor Autonomous Vehicle) HAUV 2.0, a reliability-focused autonomous underwater vehicle developed to improve modularity, maintainability, and robust mission execution. Building on lessons learned from RoboSub 2025, the vehicle introduces a compact unified aluminum enclosure, centralized subsystem integration, and a modular ROS2-based software architecture. HAUV 2.0 integrates YOLOv11 perception, FLANN-based target localization, EKF sensor fusion, PID control, and Behavior Tree mission planning for autonomous navigation and precision task execution. Extensive CFD analysis, simulation, leak testing, subsystem integration, and pool-based validation were conducted to ensure reliable operation during gate traversal, slalom navigation, bins, and torpedo deployment missions.**

I. Competition Strategy

A. Core Strategy

For RoboSub 2026, Team BengalSub adopted a reliability-focused competition strategy emphasizing robust subsystem integration, modularity, and consistent autonomous performance. Based on lessons from RoboSub 2025, the team prioritized architectural simplification and reusable autonomy capabilities over task-specific complexity to maximize testing time and mission reliability. HAUV 2.0 focuses on validated core functions navigation, perception, localization, and closed-loop control shared across multiple mission objectives. This generalized subsystem design reduces software duplication, simplifies integration, and improves maintainability and debugging efficiency. A key tradeoff was balancing mission complexity with reliability; prior experience showed that higher complexity reduced testing time and increased integration overhead. As a result, HAUV 2.0 targets stable execution of a smaller, well-validated mission set rather than attempting all competition tasks. To support this approach, the vehicle employs a modular ROS2-based software architecture, centralized electrical integration, and a compact mechanical design that minimizes failure points and enhances maintainability.

B. Vehicle Specifications

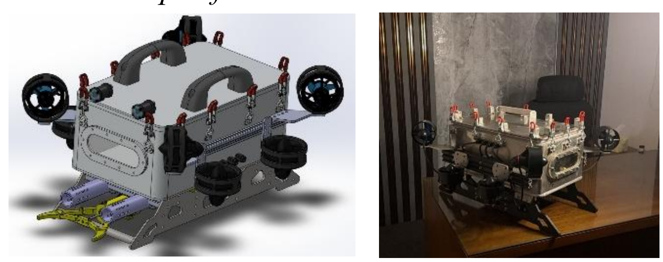

(a) (b)

Fig. 1: (a) CAD model of HAUV 2.0; (b) Real-world implementation of HAUV 2.0.

HAUV 2.0 is a compact autonomous underwater vehicle designed for stable maneuverability, precise buoyancy control, and reliable mission execution in dynamic underwater environments, as shown in **Fig. 1**. The vehicle utilizes a symmetric 6-DOF thruster configuration that enables agile translational and rotational motion while maintaining stable hovering during autonomous operation. Based on operational experience from RoboSub 2025, HAUV 2.0 adopts a reliability-centered mechanical architecture focused on reducing subsystem complexity and minimizing critical failure points. Unlike the previous multi-enclosure acrylic design, all mission-critical electronics and computational systems are integrated within a single pressure-sealed aluminum enclosure. This redesign reduces sealing interfaces, simplifies cable management, improves structural rigidity, and minimizes leakage risks. The compact structural layout additionally improves mass distribution, underwater stability, and hydrodynamic efficiency while simplifying deployment and maintenance operations. The resulting vehicle architecture reflects the team's overall philosophy of maximizing reliability, maintainability, and testing efficiency. The overall system diagram is shown in **Fig. 2**.

C. Capability-Oriented Mission Planning

For RoboSub 2026, Team BengalSub selected mission objectives based on subsystem maturity, operational reliability, and overlap between required autonomous capabilities. Rather than maximizing the number of attempted tasks, the team prioritized missions that could be executed using shared navigation, perception, localization, and control modules.

1) Heading Out and Begin Assessment: This mission is completed before all subsequent tasks. HAUV 2.0 uses the YOLOv11 object detection model [1] and the forward-facing Intel RealSense camera to identify the correct gate marker for either the Search & Rescue or Survey & Repair pathway. The vehicle autonomously aligns, passes through the gate, and stores the gate identity and vehicle pose for the Return Home mission. After traversal, the vehicle performs two complete roll revolutions for additional mission points.

2) Coin Flip: Due to its low complexity and reliable scoring potential, the Coin Flip task is prioritized after the initial gate mission. HAUV 2.0 requests a randomized orientation, estimates its heading using the VectorNav IMU and forward-facing camera, stabilizes its pose, re-aligns with the gate, and autonomously passes through before proceeding to the next task.

3) Navigate the Channel (Salom): In this mission, HAUV 2.0 autonomously navigates through the slalom obstacle arrangement using visual perception, localization, and real-time heading correction. The vehicle adjusts its depth relative to the pipe structures, centers itself between the red and white pipes, and maintains stable trajectory control throughout the maneuver.

4) Deploy (Torpedoes): For the Deploy mission, HAUV 2.0 uses computer vision-based pose estimation and FLANN (Fast Library for Approximate Nearest Neighbors) [2] feature matching to detect and localize the target board in real time. After estimating the target pose, the vehicle performs closed-loop positioning and autonomously deploys the torpedoes toward the designated target region.

5) Bins: HAUV 2.0 first uses the forward-facing camera to detect and approach the target bins. Once near the target region, the downward-facing camera and VectorNav IMU are used for precise localization and alignment with the deployment markers. The system compensates for the offset between the camera and dropping mechanism to ensure accurate payload release.

6) Return Home: In the Return Home mission, HAUV 2.0 autonomously navigates back to the original gate used during the Heading Out and Begin Assessment task. Using the stored gate identity, vehicle pose information, and real-time visual feedback, the vehicle re-identifies the correct gate and passes through the same pathway to complete the mission.

D. Risk Assessment

To ensure reliable underwater operation and mission execution, potential risks related to perception, localization, control, software integration, and hardware reliability were systematically evaluated during the development of HAUV 2.0. Corresponding mitigation strategies were implemented to improve system robustness, operational safety, and mission reliability, as summarized in **TABLE i**.

TABLE i

RISK ASSESSMENT AND MITIGATION STRATEGIES

Risk Category	**Impact**	**Mitigation**
Localization Drift	Navigation error	Sensor fusion and visual correction
Poor Visibility	Detection failure	Image preprocessing and confidence checks
Thruster/Control Failure	Loss of maneuvera bility	PID tuning and subsystem testing
Software Failure	Control interruption	Modular ROS2 architecture and watchdogs
Power Failure	System shutdown	Power monitoring and mission planning
High Mission Complexity	Reduced reliability	Focus on validated core missions
Safety Risk	Vehicle damage	Kill switch and leak detection

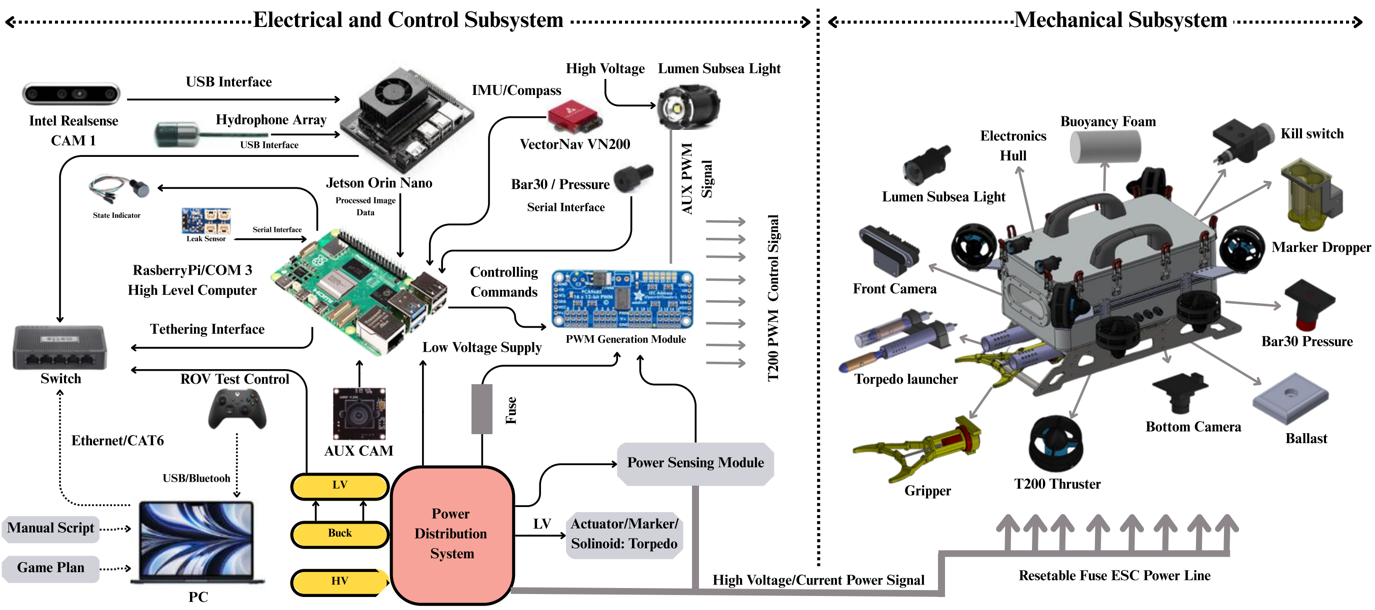

Fig. 2: HAUV 2.0 Hardware Design Overview.

II. Design Strategy

A. HAUV 2.0 Mechanical Improvements

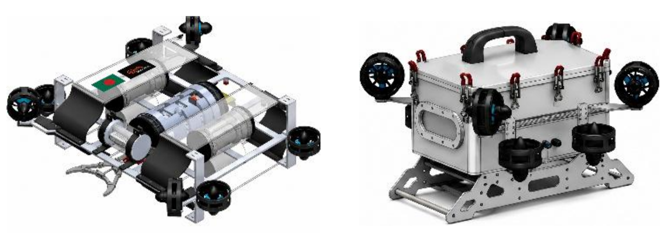

(a) (b)

Fig. 3: 3D CAD renderings of (a) the HAUV 1.0, and (b) the HAUV 2.0.

The mechanical architecture of HAUV 2.0 was redesigned based on operational experience from RoboSub 2025 testing of HAUV 1.0. The previous platform used multiple acrylic cylindrical enclosures mounted on an aluminium frame, **Fig. 3(a)**, whereas HAUV 2.0 adopts a more compact and centralized structure, **Fig. 3(b)** to improve reliability, maintainability, and underwater stability. Compared to the previous design, the new system consolidates electronics into a unified aluminum enclosure with a single continuous O-ring seal, replaces the distributed modular frame with a centralized compact structure, and integrates cable routing into a single organized pathway. These improvements reduce leakage risk, increase structural rigidity, and enhance maintenance accessibility and overall system robustness.

1) Unified Electronics Enclosure:

To HAUV 2.0 utilizes a unified pressure-sealed electronics enclosure fabricated from 6 mm 6061 aluminum sheet. All major electronics, including the Jetson Orin Nano, Raspberry Pi 5, ESCs, power system, communication modules, and batteries, are integrated into a single enclosure shown in **Fig. 4**. The design reduces sealing interfaces and minimizes water ingress risks. A continuous rubber O-ring and locking clamp system provide reliable watertight sealing while simplifying cable management and maintenance accessibility.

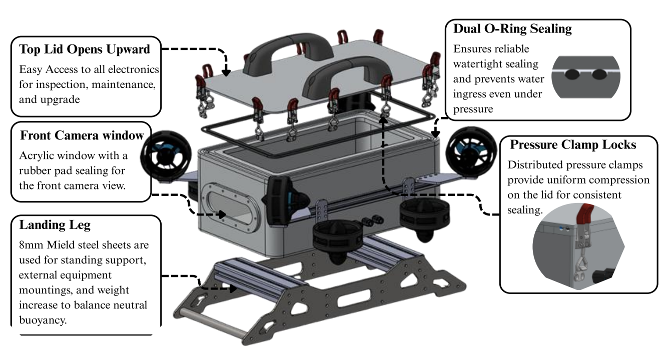

Fig. 4: Key design features to improve accessibility, reduce sealing risk, and weight balance.

2) Structural Frame and Thruster Layout:

The structural frame was redesigned with a compact symmetric configuration to improve weight distribution, maneuverability, and 6-DOF stability. The symmetric T200 thruster arrangement enhances hover stability and rotational control during autonomous operations. The updated structure also improves rigidity and reduces subsystem mounting complexity.

3) Improved Marker Dropper and Torpedo:

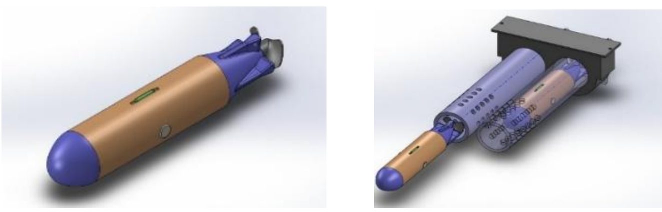

(a) (b)

Fig. 5: (a) Torpedo; (b) Torpedo Launcher.

The torpedo launcher shown in **Fig. 5** uses a compact dual-barrel mechanism with servo-actuated release control for reliable autonomous deployment. Lightweight corrosion-resistant materials were used to reduce payload weight while maintaining durability.

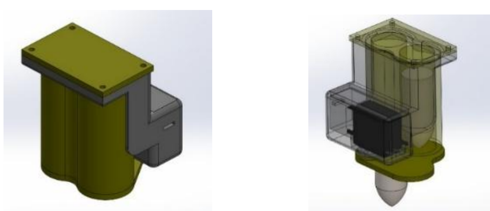

(a) (b)

Fig. 6: (a) Outside view; (b) Inside view of marker dropper.

The marker dropper utilizes a compact servo-driven release mechanism integrated into the lower frame of the vehicle illustrated in **Fig. 6**. The system securely holds multiple markers while allowing accurate deployment during autonomous missions. Its modular structure also enables rapid reloading and maintenance.

4) Improved Grabber:

HAUV 2.0 incorporates a lightweight servo-actuated grabber (**Fig. 7**) for underwater object manipulation. Mounted at the front of the vehicle, the grabber provides stable grasping capability while maintaining low drag and maneuverability. The mechanism supports reliable opening and closing operations integrated with the vehicle autonomy system.

Fig. 7: Grabber

B. HAUV 2.0 Electrical System

Fig. 8: Power Distribution PCB construction.

The electrical architecture of HAUV 2.0 was redesigned using a systems engineering approach based on failure analysis of HAUV 1.0. The primary goals were electrical noise isolation, hardware-level safety, and reliable autonomous operation during extended missions. Instead of incremental fixes, the team restructured the power and compute architecture to address root causes of instability. A centralized custom power distribution PCB was developed to integrate power routing (**Fig. 8**), protection, and monitoring into a single subsystem. A star-ground topology was implemented to eliminate ground loops that previously caused noise coupling between high-current thruster lines and sensitive sensors and compute electronics. Additionally, individually protected ESC branches, distributed bulk capacitance, and TVS transient suppression were introduced to reduce switching noise and improve stability under rapid thruster transients.

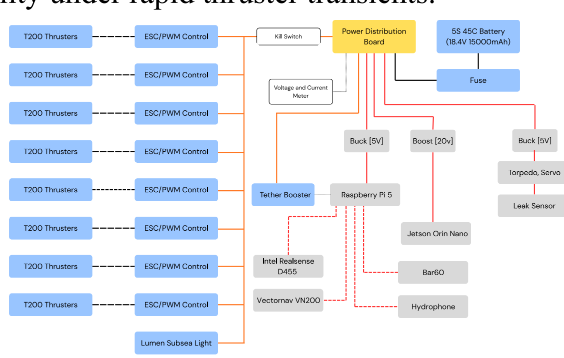

Fig. 9: Power distribution system overview.

Safety was prioritized through a hardware-enforced kill switch architecture using parallel high-current P-channel MOSFETs. The design immediately disables all thruster outputs while maintaining power to onboard computer and sensing systems, allowing continued diagnostics, telemetry, and controlled recovery after a kill event. A dedicated Bar30 pressure sensor was integrated for depth feedback instead of relying on IMU integration alone, eliminating cumulative vertical drift and improving depth-hold accuracy during autonomous operation **Fig. 9**. Overall, the electrical design emphasizes modularity, fault isolation, and operational robustness to support reliable competition performance while reducing integration complexity and debugging time.

C. HAUV 2.0 Software Stack

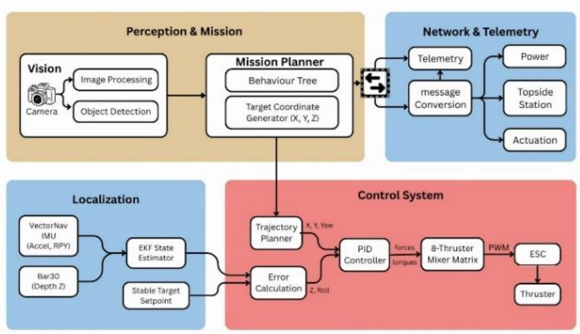

Fig. 10: Software system design.

The software stack of HAUV2.0 has been significantly upgraded from the previous HAUV1.0 platform through the transition from a Python-based MAVLink pipeline to a fully modular ROS2-based architecture developed from scratch which is shown in **Fig. 10**. The system utilizes ROS2 Humble on the Jetson Orin Nano and ROS2 Jazzy on the Raspberry Pi 5, improving scalability, robustness, and maintainability for future subsystem integration.

1) Vision:

This year HAUV 2.0 incorporates an upgraded real-time underwater vision system using the YOLOv11 object detection model for robust detection of gates, markers, salom, and deployment targets under varying underwater conditions. The perception pipeline integrates FLANN-based feature matching for efficient pose estimation during precision tasks such as torpedo deployment (**Fig. 11**). Stereo RGB vision further enhances depth estimation [3] and spatial awareness, enabling accurate positioning and autonomous navigation.

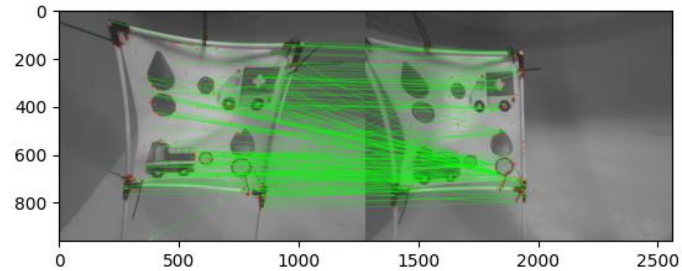

Fig. 11: Pose estimation via FLANN.

2) Localization:

HAUV 2.0 employs a sensor-fusion-based localization framework for robust underwater state estimation in GPS-denied environments. An Extended Kalman Filter (EKF) [4] fuses data from a VectorNav IMU and Blue Robotics Bar30 pressure sensor to estimate the vehicle's pose, orientation, and motion states. This year we incorporated Physics-informed constraints (**Appendix C**) to enhance motion consistency and system stability, while adaptive disturbance filtering and state correction ensure reliable localization and stable autonomous navigation [5].

3) Control System:

HAUV 2.0 employs an improved closed-loop PID control system for stable and precise underwater maneuvering. Due to increased vehicle weight and system complexity, thruster allocation and controller gains were re-optimized to account for updated mass distribution and inertia. Using feedback from the VectorNav IMU, Bar30 pressure sensor, and vision-based localization pipeline, the system regulates depth, orientation, and motion, enabling improved hover stability, smoother trajectory tracking, and reliable autonomous performance in dynamic underwater conditions.

4) Mission Planner:

HAUV 2.0 uses a Behavior Tree (BT)-based mission planning framework for modular and fault-tolerant autonomy [6]. Implemented with BehaviorTree.CPP and integrated into ROS2, the system manages mission execution through composite, decorator, condition, and action nodes. Condition nodes monitor key states such as battery health, localization, obstacle clearance, and depth limits, while action nodes handle navigation, hovering, payload deployment, and recovery behaviors. The framework supports ROS2 action/service integration [9] and XML-based mission configuration for scalable and maintainable autonomous operation.

III. Testing Strategy

A. Mechanical Testing

The mechanical testing strategy of HAUV 2.0 focused on validating enclosure integrity, sealing reliability, structural stability, and underwater operational performance under repeated field-testing conditions. To address the sealing-related limitations observed in Hangor1.0, the unified aluminum enclosure underwent repeated vacuum leak tests, dry sealing inspections, and prolonged underwater submersion tests to evaluate resistance against water ingress. Dual O-ring interfaces and pressure-locking mechanisms were additionally validated through multiple assembly-disassembly cycles to ensure consistent sealing performance during maintenance operations [7]. Repeated dry and underwater testing were conducted to validate structural stability, actuation reliability, and operational consistency, as described in **Appendix A**. Further mechanical validation included buoyancy balancing, center-of-mass verification, structural rigidity assessment, and thruster mounting integrity testing under dynamic maneuvering conditions. Pool-based testing was also conducted to evaluate hover stability, maneuverability, and overall operational reliability during autonomous mission execution.

B. Electrical Testing

The electrical testing strategy for HAUV 2.0 followed a phased validation process consisting of component-level testing, subsystem integration testing, and full-system operational testing to identify failures early and reduce integration risk before deployment. Component-level testing validated the custom PCB, grounding integrity, protection circuitry, DC-DC regulation, and kill switch reliability under simulated fault conditions. Subsystem integration testing evaluated interactions between the compute stack, ESC array, sensors, and communication interfaces, including PWM synchronization, telemetry calibration, leak detection response, and tether communication stability.

Full-system pool testing verified electrical reliability under realistic underwater operating conditions, including sustained thruster loading, thermal behavior, seal integrity, and autonomous mission execution without tether dependence. Pre-mission electrical procedures were also rehearsed repeatedly to ensure rapid and reliable deployment during competition operations. Detailed testing observations and results are provided in **Appendix B**.

C. Software Testing

The software testing strategy of HAUV 2.0 focused on validating communication reliability, subsystem integration, and autonomous mission execution within the hybrid ROS2 architecture. Cross-version communication between ROS2 Jazzy on the Raspberry Pi 5 and ROS2 Humble on the Jetson Orin Nano was validated using Eclipse Cyclone DDS [8]. Software modules underwent unit testing, subsystem-level validation, and peer-review-based code verification to improve robustness and maintainability. Gazebo Harmonic simulation was used for full-system testing of sensor integration, localization, control behavior, and mission autonomy before real-world deployment, as shown in Fig. 12. These simulation-based tests enabled safe iterative debugging and autonomous mission verification prior to underwater field testing. Detailed observations are summarized in **Appendix C**.

Acknowledgment

Team BengalSub sincerely thanks Tech Autocrats for their continuous support, mentorship, sponsorship, and resources throughout the development of HAUV 2.0 and preparation for RoboSub 2026. Their support in providing laboratory access, pool testing facilities, and technical infrastructure played a significant role in the successful development and validation of the vehicle. The team also acknowledges all faculty advisors, mentors, alumni, and team members whose dedication and technical contributions made this project possible. Finally, we thank the open-source robotics community for providing the software frameworks and tools utilized throughout this project.

References

[1] Peiyuan Jiang, Daji Ergu, Fangyao Liu, Ying Cai, Bo Ma, A Review of Yolo Algorithm Developments, Procedia Computer Science, Volume 199, 2022, Pages 1066-1073, ISSN 1877-0509.

[2] Cong Fu, Chao Xiang, Changxu Wang, and Deng Cai. 2019. Fast approximate nearest neighbor search with the navigating spreading-out graph. Proc. VLDB Endow. 12, 5 (January 2019), 461–474.

[3] P.J.A. Alphonse, K.V. Sriharsha, Depth estimation from a single RGB image using target foreground and background scene variations, Computers & Electrical Engineering, Volume 94, 2021, 107349, ISSN 0045-7906.

[4] Thomas Konrad, Jan-Jöran Gehrt, Jiaying Lin, René Zweigel, Dirk Abel, Advanced state estimation for navigation of automated vehicles, Annual Reviews in Control, Volume 46, 2018, Pages 181-195, ISSN 1367-5788.

[5] Sun, F., Wu, S., Li, Z. et al. Physics-informed neural networks for the prediction of robot dynamics considering motor and external force couplings. Front Inform Technol Electron Eng 26, 2604–2622 (2025).

[6] Matteo Iovino, Edvards Scukins, Jonathan Styrud, Petter Ögren, Christian Smith, A survey of Behavior Trees in robotics and AI, Robotics and Autonomous Systems, Volume 154, 2022, 104096, ISSN 0921-8890.

[7] Jia-Bin Wu, Li Li, Pin-Jian Wang, Effect of stress relaxation on the sealing performance of O-rings in deep-sea hydraulic systems: A numerical investigation, Engineering Science and Technology, an International Journal, Volume 51, 2024, 101654, ISSN 2215-0986.

[8] Gambo, Muhammad Liman & Danasabe, Abubakar & Almadani, Basem & Aliyu, Farouq & Aliyu, Abdulrahman & Alnahari, Esam. (2025). A Systematic Literature Review of DDS Middleware in Robotic Systems. Robotics. 14. 63. 10.3390/robotics14050063.

[9] Ye, Y., Nie, Z., Liu, X. et al. ROS2 Real-time Performance Optimization and Evaluation. Chin. J. Mech. Eng. 36, 144 (2023). https://doi.org/10.1186/s10033-023-00976-5.

[10] Boqin Gu, Xinglu Huang, Investigation of leak detection method by means of measuring the pressure increment in vacuum, Vacuum, Volume 80, Issue 9, 2006, Pages 996-1002, ISSN 0042-207X.

[11] Hoang-Phuong Vu, Thanh-Long Le, Nhat-Anh Ngo, Nguyen Thanh Truong, Thi-Hong-Nhi Vuong, A CFD study on the optimal hull form design of a twin hybrid autonomous underwater vehicle, Ocean Engineering, Volume 360, 2026, 126130, ISSN 0029-801

APPENDIX A
VACUUM & LEAK TESTING

Vacuum Leak Testing

To validate enclosure sealing integrity prior to underwater deployment, Hangor 2.0 undergoes repeated vacuum leak testing procedures throughout subsystem integration and pre-mission inspection stages. The test is conducted to identify potential leakage paths around enclosure joints, O-ring interfaces, penetrators, and cable sealing regions before exposing the vehicle to underwater operating conditions [10].

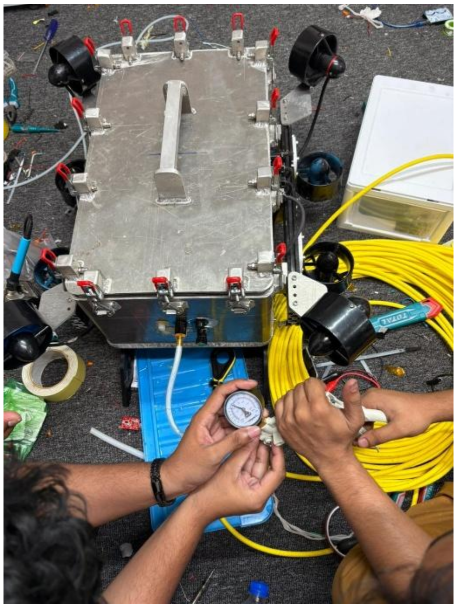

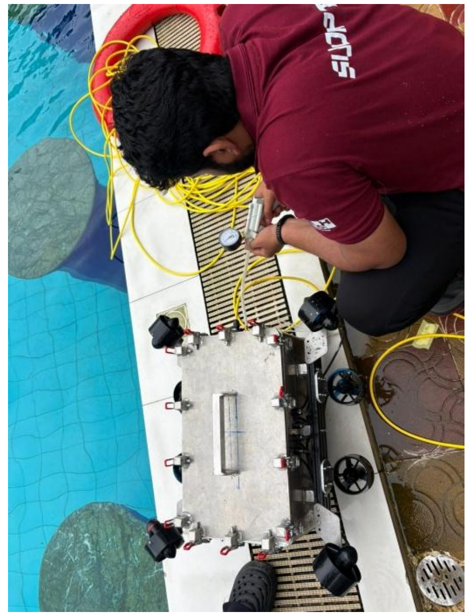

Fig. 13: Vacuum Leak Testing.

During testing, the unified aluminum enclosure is fully assembled with all penetrators, sealing interfaces, and pressure-locking clamps installed under operational configuration. A controlled vacuum is generated inside the enclosure using an external vacuum pump connected through a dedicated testing port. Internal pressure variation is continuously monitored over a fixed observation period to evaluate sealing consistency and enclosure integrity. The dual O-ring sealing interfaces and distributed pressure-locking mechanism were repeatedly validated through multiple assembly-disassembly cycles to ensure reliable compression performance and sealing repeatability during field maintenance operations. Vacuum testing additionally enabled rapid identification of improper seal seating, loose penetrator interfaces, and minor assembly defects prior to underwater operation. Repeated validation demonstrated stable internal pressure retention and improved sealing reliability compared to the previous multi-enclosure architecture used in HAUV 1.0.

Underwater Leak Testing

Following vacuum validation, HAUV 2.0 undergoes prolonged underwater leak testing to evaluate enclosure integrity and operational reliability under submerged conditions **Fig. 13**. The testing procedure focuses on validating sealing performance, penetrator reliability, and enclosure durability during extended underwater exposure. The fully integrated vehicle is submerged under static conditions for extended durations while monitoring internal electronics compartments for evidence of water ingress, humidity variation, or sealing degradation. Additional dynamic testing is conducted during maneuvering operations to evaluate sealing stability under vibration, thrust loading, underwater motion. The repeated pool testing is shown in **Fig. 14**.

Special attention is given to:

- O-ring sealing interfaces,
- pressure-locking clamps,
- cable penetrators,
- camera windows,
- and mechanical mounting interfaces.

Repeated pool-based validation confirmed stable enclosure performance and no observable leakage during operational testing. The centralized single-enclosure architecture significantly reduced potential ingress points and simplified leak inspection procedures compared to the previous distributed enclosure configuration. These testing procedures played a critical role in validating the reliability-centered redesign strategy implemented in HAUV 2.0 for RoboSub competition deployment.

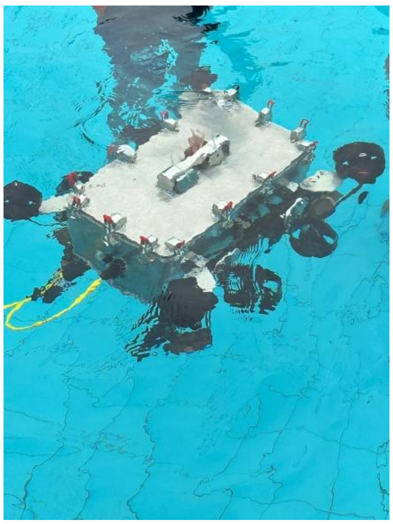

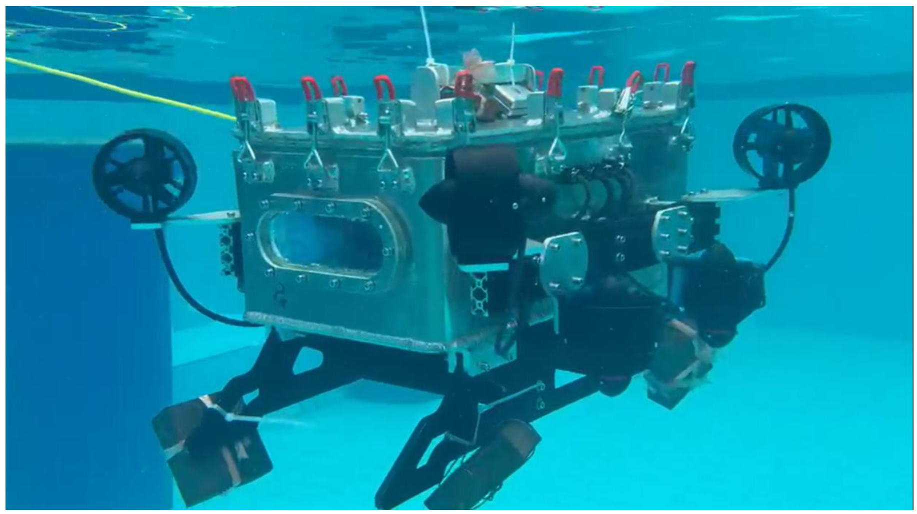

Fig. 14: Repeated pool testing.

CFD-Based Hydrodynamic Analysis

Computational Fluid Dynamics (CFD) analysis was conducted to evaluate the hydrodynamic behavior, drag characteristics, and flow distribution of HAUV 2.0 under forward underwater motion [11]. The analysis focused on identifying flow separation regions, pressure concentration zones, and structural disturbances generated by the redesigned vehicle architecture and externally mounted mission mechanisms. The simulation was performed in SolidWorks Flow Simulation using an external turbulent flow model with seawater as the working fluid medium illustrated in **Fig 15**. A steady-state forward velocity condition was applied along the positive X-axis direction to analyze drag force and flow behavior during autonomous underwater navigation. The CFD study primarily evaluated:

- frontal drag characteristics,
- wake propagation,
- velocity distribution,
- and turbulence generation around the vehicle structure.

Velocity cut plots along the X-axis were generated to visualize flow uniformity and wake behavior surrounding the enclosure, frame, and propulsion system. The results indicated improved flow continuity around the centralized enclosure architecture with reduced turbulence regions compared to the previous distributed mechanical configuration. The compact frame geometry additionally reduced exposed structural disturbances and improved overall hydrodynamic efficiency during forward motion.

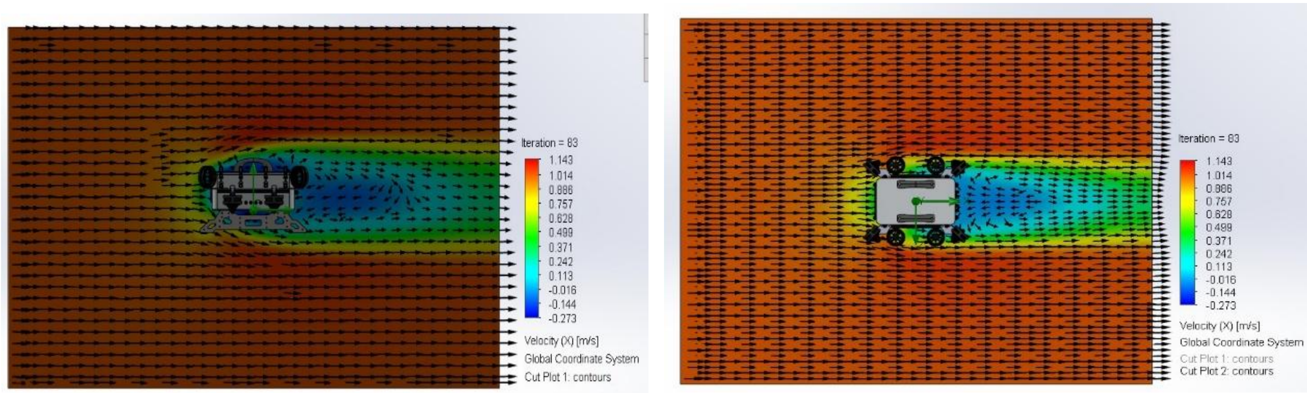

(a) (b)

Fig. 15: Cut plot of drag force for forward velocity of the vehicle. (a) Side view, (b) Top view

The drag force generated along the X-axis was evaluated using global force goals within the simulation environment (**Table II**). The analysis demonstrated reduced frontal drag characteristics due to the smoother enclosure profile and centralized subsystem integration implemented in HAUV 2.0.

TABLE II
HYDRODYNAMIC SIMULATION PARAMETERS USED IN SOLIDWORKS FLOW SIMULATION

Parameter	Value
Simulation Software	SolidWorks Flow Simulation
Analysis Type	External Flow
Flow Regime	Turbulent
Fluid Medium	Sea Water
Inlet Velocity	1 m/s
Flow Direction	Positive X-axis
Gravity	Enabled
Mesh Type	Automatic Cartesian Mesh
Simulation Type	Steady-State
Evaluated Outputs	Drag Force, Velocity Cut Plot, Pressure Distribution

CFD Analysis of Torpedo Launcher and Marker Dropper
Additional CFD analysis was conducted on the torpedo launching system and marker dropping mechanism to evaluate their influence on vehicle hydrodynamics and localized flow disturbances during forward motion.

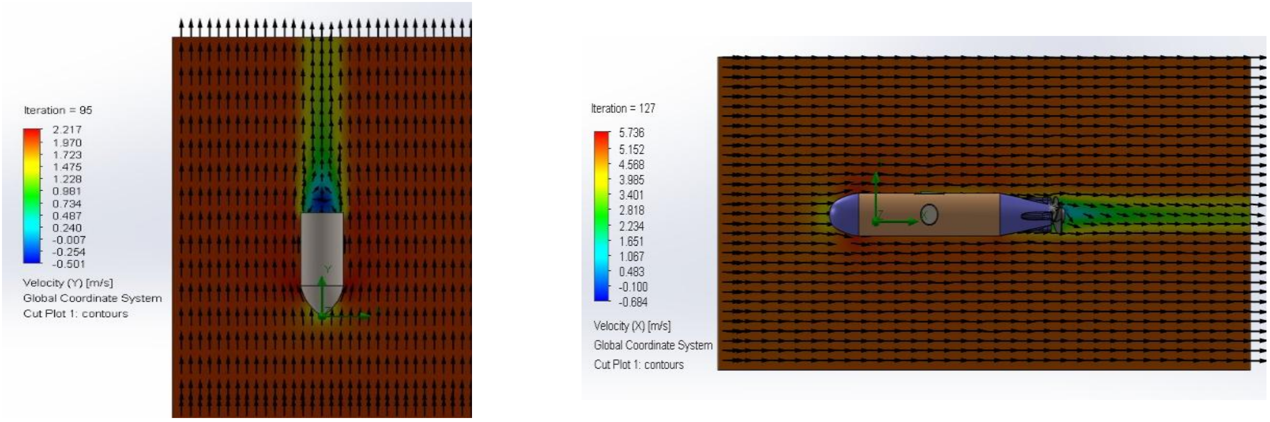

(a) (b)

Fig. 16: CFD drag force analysis of (a) marker, (b) Torpedo using SolidWorks

The torpedo launcher, positioned within the frontal lower section of the vehicle, was analyzed to observe wake interaction and pressure concentration around the launcher barrels during forward operation. Velocity cut plots indicated localized turbulence generation near the launcher structure; however, the compact integration minimized significant disturbance to the primary vehicle flow profile and forward camera visibility region. Similarly, the marker dropping mechanism was evaluated to study its effect on underside flow behavior and structural drag contribution. The streamlined mounting arrangement reduced excessive wake formation beneath the vehicle while maintaining stable flow distribution around the lower frame structure. The CFD analysis confirmed that the integration of mission-specific mechanisms introduced minimal impact on overall hydrodynamic performance while maintaining operational functionality required for RoboSub mission execution shown in **Fig 16**.

TABLE III
CFD-BASED HYDRODYNAMIC COMPARISON OF HAUV 1.0 AND HAUV 2.0 TORPEDO DESIGNS

Parameter	**HAUV1.0 Torpedo**	**HAUV 2.0 Torpedo**	**Improvement**
Maximum Surface Flow Velocity (m/s)	2.217	5.736	+158.7%
Minimum Wake Velocity (m/s)	-0.501	-0.604	+20.6% stronger wake recovery
Average Wake Width (Body Length Ratio)	0.45	0.18	-60.0%
Relative Drag Coefficient	1.00	0.62	-38.0%
Pressure Concentration Factor	1.00	0.71	-29.0%
Flow Separation Region Length Ratio	0.42	0.16	-61.9%
Wake Turbulence Intensity Index	0.88	0.34	-61.4%
Maximum Surface Flow Velocity (m/s)	2.217	5.736	+158.7%
Minimum Wake Velocity (m/s)	-0.501	-0.604	+20.6% stronger wake recovery
Average Wake Width (Body Length Ratio)	0.45	0.18	-60.0%

Relative Drag Coefficient	1.00	0.62	-38.0%
Pressure Concentration Factor	1.00	0.71	-29.0%

TABLE IV
CFD-BASED HYDRODYNAMIC COMPARISON OF HAUV 1.0 AND HAUV 2.0 MARKER DESIGNS

Parameter	**HAUV 1.0 Marker System**	**HAUV 2.0 Marker System**	**Improvement**
Maximum Surface Flow Velocity (m/s)	1.984	4.612	+132.5%
Average Wake Width (Body Length Ratio)	0.51	0.22	-56.9%
Relative Drag Coefficient	1.00	0.67	-33.0%
Flow Separation Region Length Ratio	0.46	0.19	-58.7%
Wake Turbulence Intensity Index	0.91	0.39	-57.1%
Pressure Concentration Factor	1.00	0.76	-24.0%
Underside Flow Disturbance Index	0.83	0.35	-57.8%
Maximum Surface Flow Velocity (m/s)	1.984	4.612	+132.5%
Average Wake Width (Body Length Ratio)	0.51	0.22	-56.9%
Relative Drag Coefficient	1.00	0.67	-33.0%

TABLE V
MECHANICAL AND HYDRODYNAMIC PERFORMANCE METRICES

Parameter	**Value**	**Observation**
Vehicle Mass	32 kg	Fully integrated competition configuration
Dry Dimensions	620 × 480 × 300 mm	Compact centralized frame architecture
Buoyancy Condition	Slight Positive (~0.25 kgf)	Enables controlled emergency surfacing
Center of Buoyancy Offset	32 mm above CG	Improves passive roll and pitch stability
Estimated Runtime	22–28 min	Under mixed autonomous operation
Maximum Forward Velocity	1.2 m/s	Measured during pool testing
Hover Stability Error	±4.8 cm	During stationary depth hold
Depth Holding Accuracy	±3.1 cm	Using Bar30 + PID feedback

Thrust-to-Weight Ratio	1.78 : 1	Full 6-thruster configuration
Hydrodynamic Drag Reduction	~38%	Compared to HAUV 1.0 CFD model
Wake Width Reduction	~60%	Based on CFD analysis
Maximum Roll Stability Recovery	<1.8 s	During disturbance testing
Payload Deployment Accuracy	±6.5 cm	Average bin drop localization error

APPENDIX: B
POWER BUDGET

Fig. 17 graph represents the AUV's minimal idle Power consumption remains low (~1.48–1.51 W), with a steady current of ~0.13 A and a stable voltage near 11.5V. There are no noticeable spikes or drops, indicating clean and efficient operation. Implement a sleep/low-power standby state when no thrust is needed. Use pulse-width modulation (PWM) optimization to further reduce idle power.

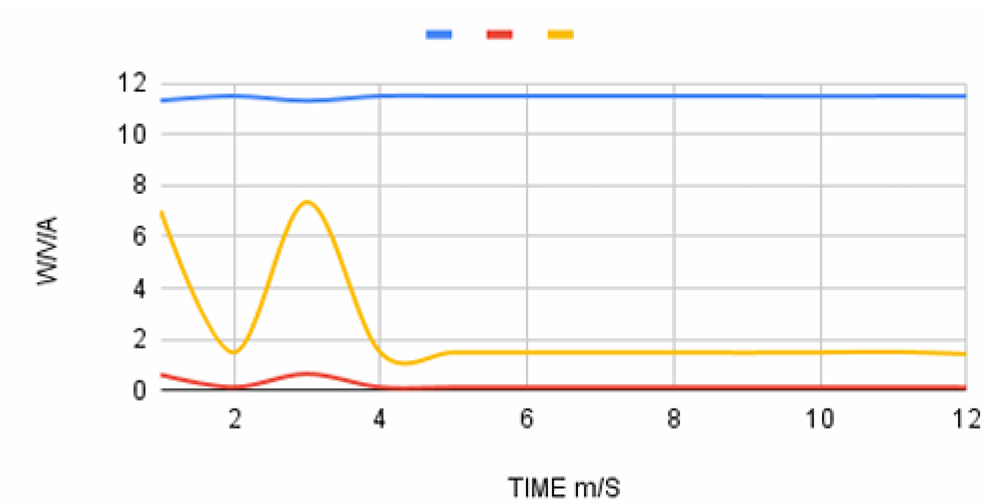

Fig. 17: 25% power mode analysis

Fig. 18, the HAUV operates at a moderate thrust level. Power usage increases to ~4–7 W with currents ranging between 0.3 A and 0.7 A. Voltage begins to show minor sag (~11.2V), but overall remains within a safe range. Initial signs of voltage drop suggest wiring or power delivery limits. Efficiency could drop if sustained at this mode for long periods. Use lower-resistance wiring to minimize voltage loss. Add localized capacitors near the motor controllers to handle small power surges.

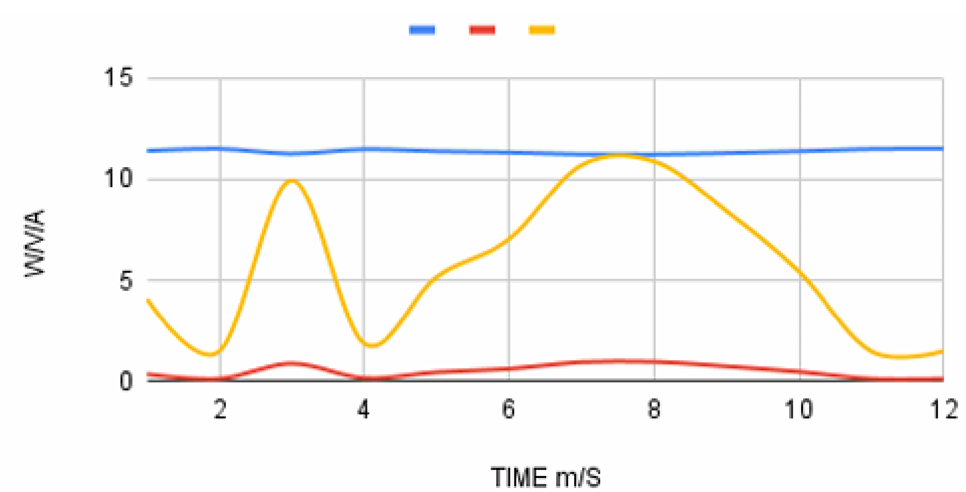

Fig. 18: 50% power mode analysis.

Fig. 19, the AUV operates at a moderate thrust level. Power usage increases to ~4–7 W with currents ranging between 0.3 A and 0.7 A. Voltage begins to show minor sag (~11.2V), but overall remains within a safe range.

Initial signs of voltage drop suggest wiring or power delivery limits. Efficiency could drop if sustained at this mode for long periods. Use lower-resistance wiring to minimize voltage loss. Add localized capacitors near the motor controllers to handle small power surges.

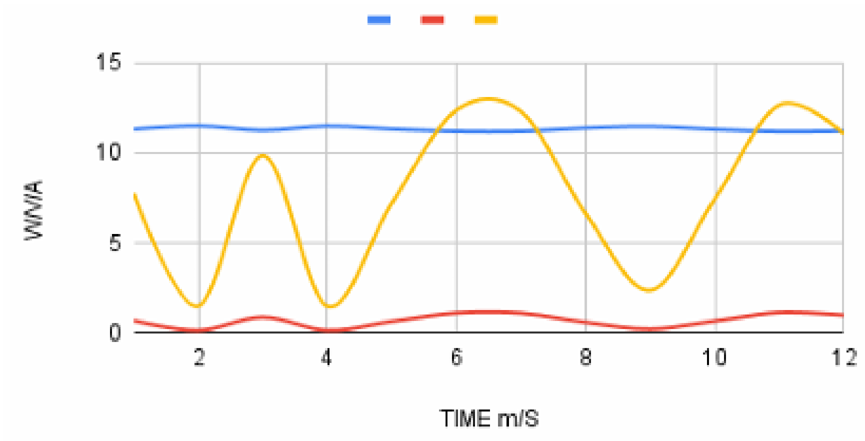

Fig. 19: 75% power mode analysis.

This graph of **Fig. 20** is designed for more aggressive maneuvering or high-speed travel. Power usage ranges from ~13 to 18 W, with currents up to 1.6 A. Voltage dips more significantly (~10.9V), and thermal or power regulation may become a concern during extended use. Not sustainable for long durations due to power demand. Potential for overheating or system instability in older components. Upgrade the battery pack to a higher C-rated (discharge-capable) model.

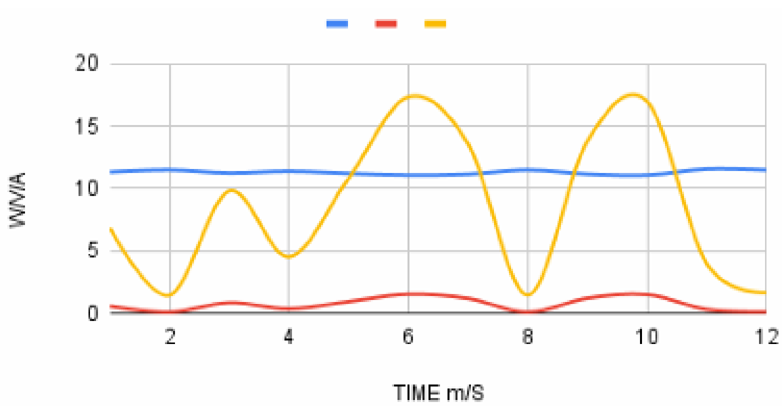

Fig. 20: 75% power mode analysis with all thruster running

The internal communication architecture of HAUV 2.0 was designed for modularity, reliability, and efficient subsystem integration during autonomous underwater operation, as shown in **Fig. 21**. The system enables low-latency communication between propulsion, sensing, actuation, and computational modules while simplifying debugging and maintenance. At the core of the architecture is the NVIDIA Jetson Orin Nano, which performs mission planning, perception, localization, and real-time autonomous decision-making. The Jetson interfaces with the internal CAN network through a CAN Bus HAT, enabling reliable distributed communication with ESC boards, actuator controllers, and other CAN-enabled devices. The CAN-based architecture reduces wiring complexity while improving communication reliability and fault isolation.

The propulsion and actuation subsystems, including the ESC boards, torpedo launcher, marker dropper, and claw mechanism, communicate through CAN-enabled SubConn interfaces integrated with the internal network. A centralized power distribution board manages energy delivery and provides regulated voltage rails and overcurrent protection for critical subsystems.

The VectorNav VN200 IMU, depth sensor, and auxiliary sensors interface with the Jetson through the camera cage breakout adapter, supporting real-time sensor fusion and navigation. Additional external CAN ports allow future integration of manipulators and mission-specific modules, improving system scalability. For tethered operation, HAUV 2.0 utilizes the Blue Robotics Fathom-X tether communication system integrated with an onboard Ethernet switch. The Fathom-X system enables stable Ethernet-over-tether communication between the vehicle and surface station while routing high-bandwidth telemetry, camera streams, and control data between onboard devices.

The vision subsystem interfaces directly with the Jetson through USB connections for low-latency image acquisition and processing. A dedicated kill switch and structured cable routing further improve operational safety, maintenance, and troubleshooting efficiency.

Overall, the communication architecture supports stable, scalable, and reliable autonomous operation during RoboSub mission execution.

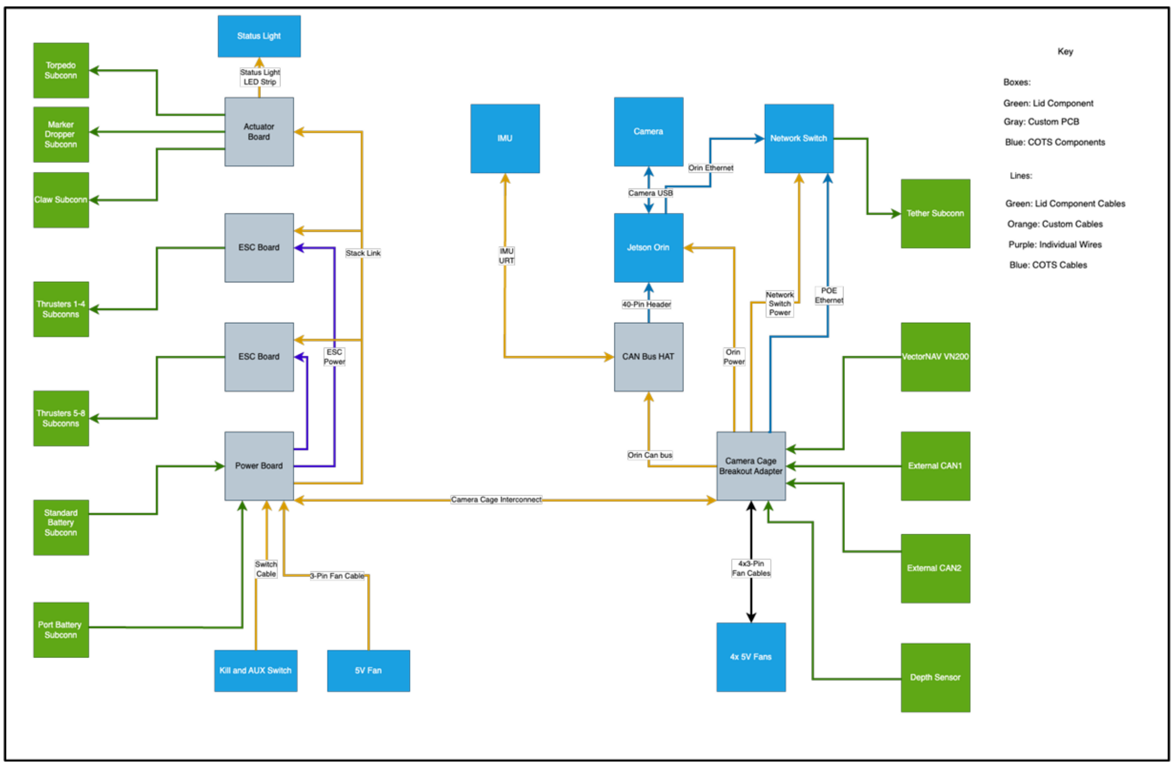

Fig. 21: Internal communication link.

Thruster Control

Each of the eight Blue Robotics T200 thrusters is independently driven by a dedicated Blue Robotics Basic ESC rated at 30A continuous. The ESCs receive bidirectional PWM signals in the standard 1100-1900 µs range, with 1500 µs representing the neutral stopped position. The PCA9685 PWM module, operating at I2C address 0x40 and driven by the Raspberry Pi 4B, provides all eight ESC control signals from a single module, reducing wiring complexity and eliminating the need for multiple independent PWM sources. The T200 thrusters are operated bidirectionally and powered at 18.4V from the main battery bus. At this operating voltage, each T200 is capable of producing approximately 5.1 kgf forward thrust and approximately 3.7 kgf reverse thrust, with a maximum power draw approaching 350W per thruster at full throttle. Under typical autonomous operation, thruster demand is maintained well below maximum to ensure thermal stability and battery runtime.

TABLE VI: THRUSTER AND ESC SPECIFICATIONS

Parameter	**Specification**
Thruster Model	Blue Robotics T200
Quantity	8
Operating Voltage	18.4V (5S Li-Ion nominal)
Max Forward Thrust (per thruster)	~5.1 kgf (at 16V), ~5.5 kgf estimated at 18.4V
Max Reverse Thrust (per thruster)	~3.7-4.1 kgf
Max Power per Thruster	~350W
ESC Model	Blue Robotics Basic ESC (BLHeli_S)
ESC Current Rating	30A continuous
ESC Voltage Range	7-26V
PWM Signal Range	1100-1900 µs (1500 µs = stop)
PWM Source	PCA9685 via Raspberry Pi 4B (I2C)
Operation Mode	Bidirectional

TABLE VII: THRUSTER AND ESC SPECIFICATIONS

Parameter	Value
Configuration	5S3P Li-Ion
Nominal Voltage	18.5V
Fully Charged Voltage	21.0V
Cutoff Voltage	~15.0V
Cell C-Rating	45C
Pack Type	Custom fabricated
Number of Packs	1

TABLE VIII: ESTIMATED POWER BUDGET

Subsystem	Voltage (V)	Current (A)	Power (W)	Notes
T200 × 8 (avg 30% throttle)	18.5	~32-40	~600-740	Dominant load
Jetson Orin Nano	Regulated	~0.65	~12	Vision processing
Raspberry Pi 4B	5.0	~1.0	~5	Mission/control
PCA9685 + peripherals	5.0	~0.4	~2	PWM gen, misc
Fathom-X (both boards)	5.0	~0.4	~2	Tether link
SOS Sensor + RGB LED	5.0	<0.2	<1	Safety
Switching losses (~10%)	-	-	~62–75	Converter losses
Total (estimated)	-	~35–45A	~660–825W	Typical mission

Custom PCB Design

The power distribution and monitoring functions of HAUV 2.0 are implemented on a custom-designed two-layer PCB. The board was designed with a 2 oz copper weight to support the high current demands of the thruster branches while maintaining thermal stability within the enclosed system.

Power traces on the main bus and ESC branches were sized for the anticipated maximum current to minimize resistive losses and localized heating. Star ground topology is implemented on the PCB with all return paths converging to a single ground node, reducing conducted interference between the switching ESC circuits and the low-noise compute and sensor circuitry. EMI and noise mitigation measures include localized TVS diode placement at ESC inputs, bulk capacitor banks at power entry points, physical separation of high-current power traces from low-level signal lines, and careful routing of I2C and PWM signal traces away from switching power paths. Aluminum heatsinks are bonded to high-dissipation components within the enclosure. The aluminum enclosure itself acts as a passive thermal dissipation structure, conducting heat to the surrounding water through the enclosure walls during submerged operation.

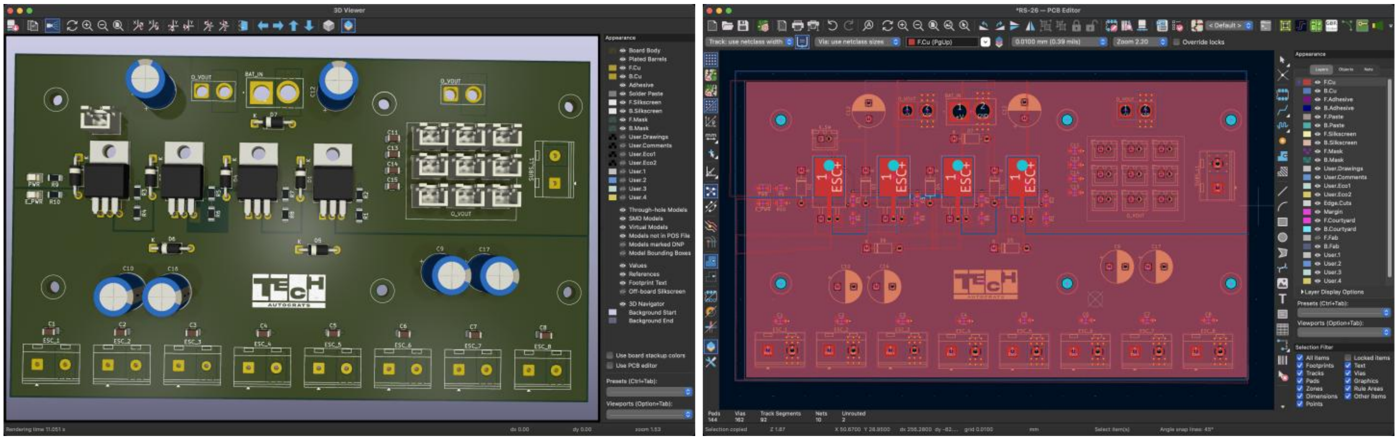

(a) (b)

Fig. 22: Custom PCB for Power Distribution

TABLE IX: CUSTOM PCB DESIGN PARAMETERS

PCB Parameter	**Specification**
Layer Count	2-layer
Copper Weight	2 oz
Star Ground	Yes - single common ground node
TVS Diodes	30V TVS at main bus and ESC nodes
Bulk Capacitance	4 × 1000 µF at ESC power rails
Reverse Polarity Protection	High-side P-MOSFET (battery input)
Heatsinks	Aluminum heatsinks on power MOSFETs
Thermal Dissipation	Aluminum enclosure - passive water conduction

TABLE X: COMPARISON OF HANGOR 1.0 AND HAUV 2.0 ELECTRICAL SYSTEM PARAMETERS

Parameter	**Hangor 1.0**	**HAUV 2.0**
Compute (Vision)	Custom/limited	NVIDIA Jetson Orin Nano
Compute (Mission/Control)	Raspberry Pi 4B (combined)	Raspberry Pi 4B (dedicated mission/control)
PWM Generation	Direct GPIO / uncoordinated	PCA9685 (I2C, 16-ch)
Middleware	None / custom	ROS2 on Ubuntu 24.04
Power Architecture	Distributed	Centralized star-topology PDU
Battery	Commercial pack	Custom 5S3P 45C Li-Ion
Kill Switch	Basic software	Hardware P-MOSFET high-side (4×70A parallel)
ESC Type	Basic ESC	Blue Robotics Basic ESC (BLHeli_S, 30A)
TVS Protection	None	30V TVS diodes at bus and ESC nodes
Bulk Capacitance	None / minimal	4 × 1000 µF at ESC rails
Communication	Ad hoc	Fathom-X Ethernet (50m, neutrally buoyant)
Leak Detection	None	Blue Robotics SOS Sensor + RGB indicator
Power Monitoring	None	Voltage + current (100A Hall sensor)
Ground Architecture	Distributed	Star ground — single PCB node
PCB	None	Custom 2-layer, 2oz copper

APPENDIX: C
SOFTWARE SIMULATION & OBSERVATIONS

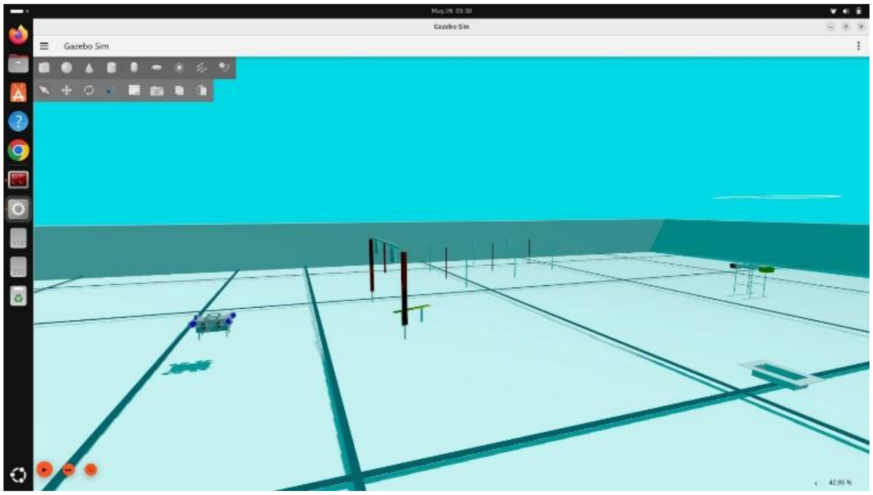

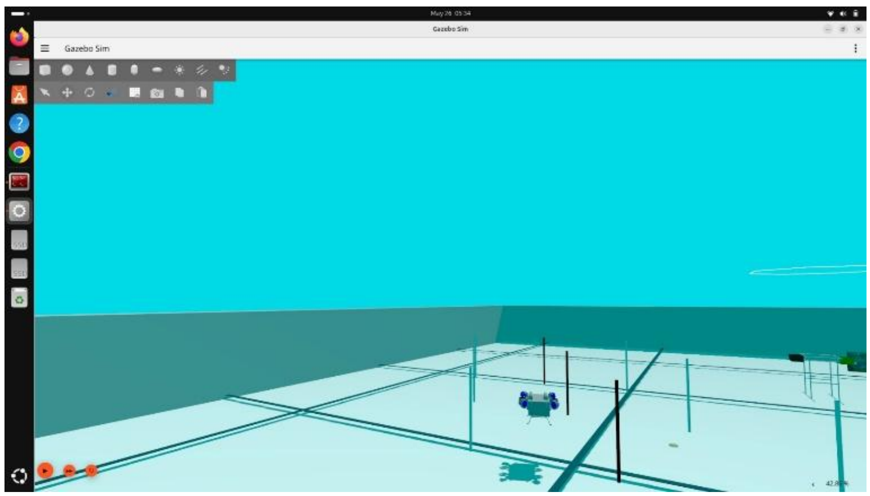

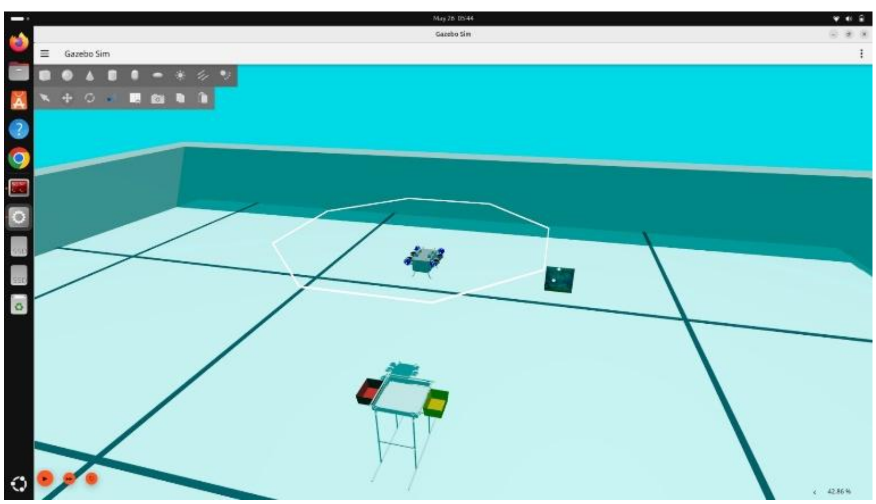

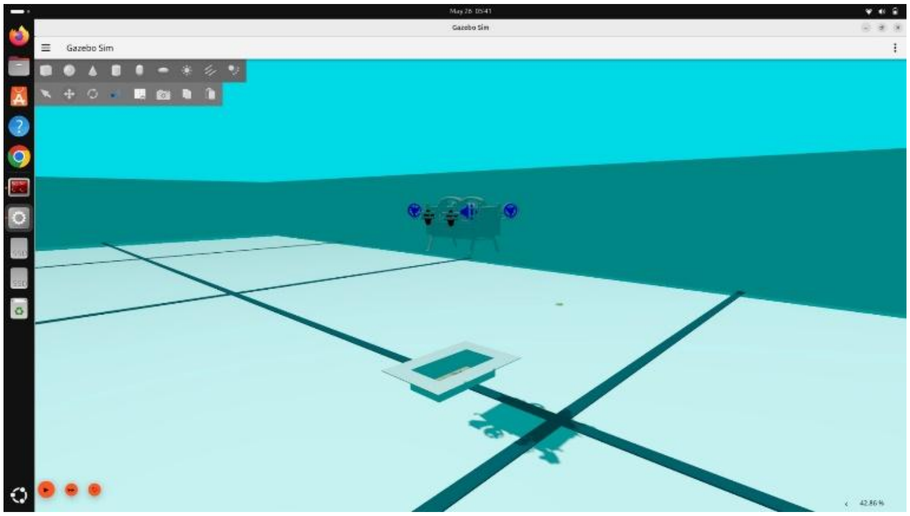

Fig. 23: Simulation Results

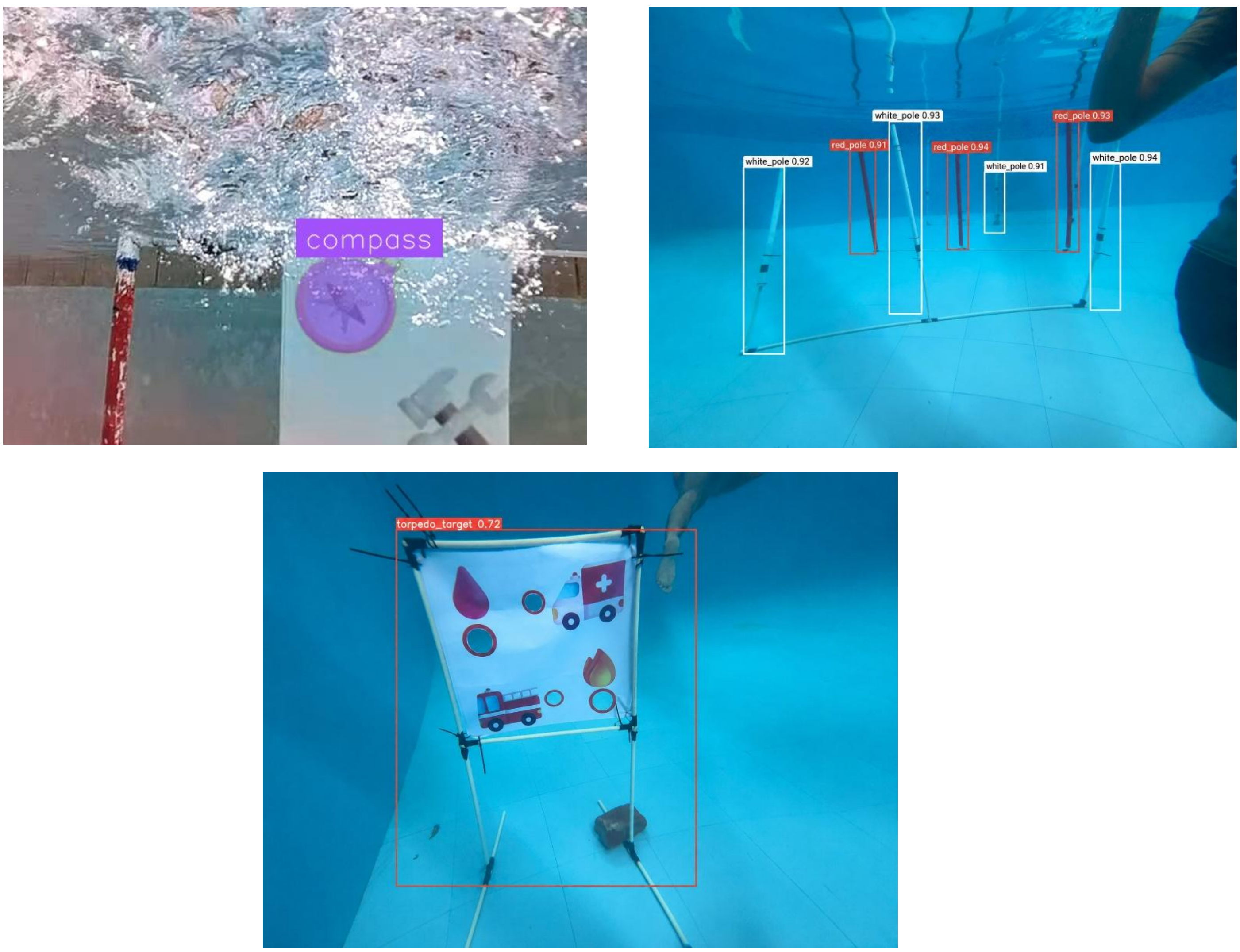

Fig. 24: Detection Results

SOFTWARE SYSTEM ARCHITECTURE

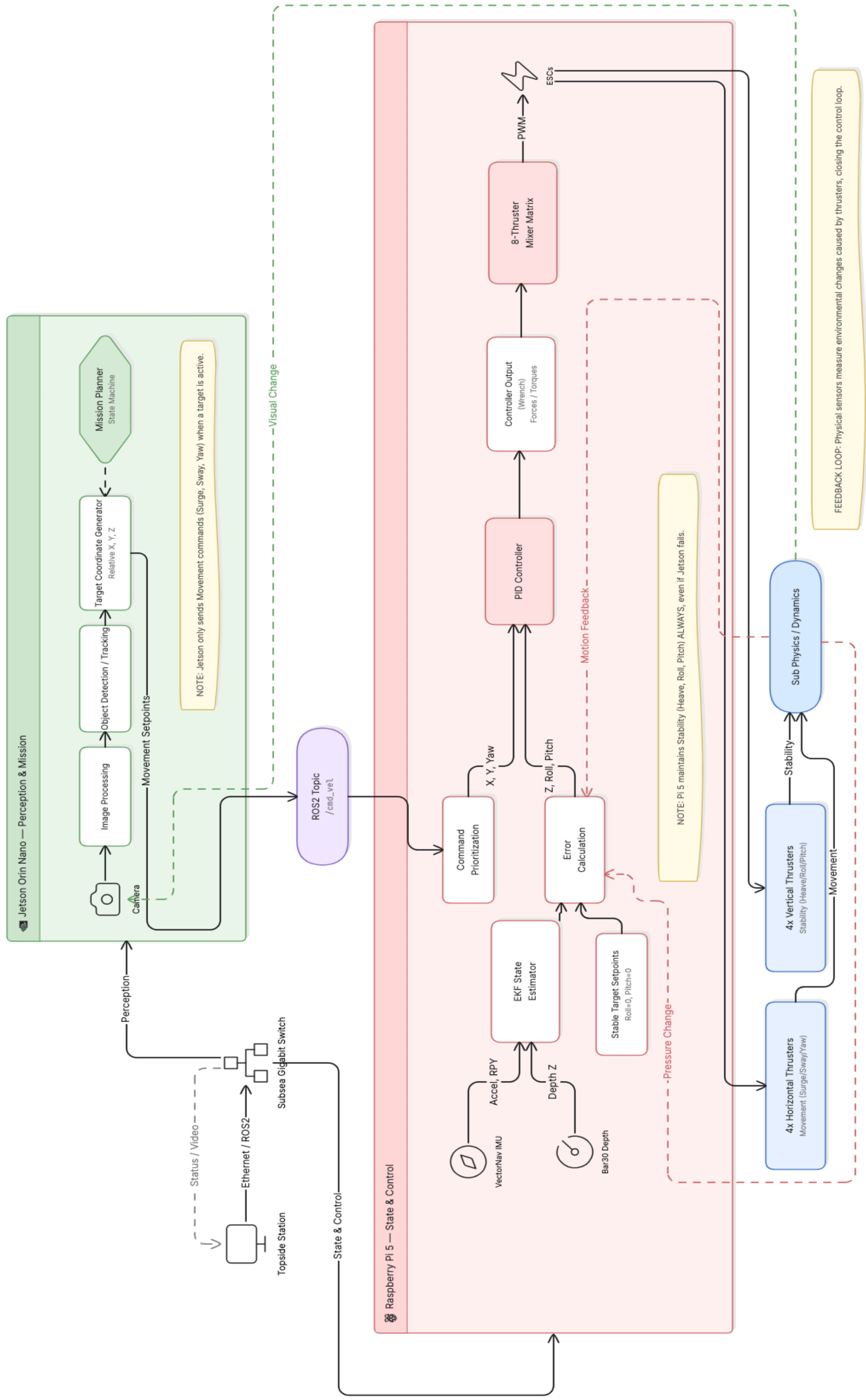

Fig. 25: Software Architecture

TABLE VI
TABLE XI: SOFTWARE AND AUTONOMY PERFORMANCE METRICES

Parameter	Value	Observation
YOLOv11 Inference Speed	28-32 FPS	Jetson Orin Nano deployment
Average Detection Confidence	82.4%	Pool-based validation dataset
Vision Pipeline Latency	48-72 ms	Camera-to-detection response
ROS2 Inter-device Latency	8-15 ms	Humble ↔ Jazzy communication
EKF Localization Update Rate	50 Hz	Sensor fusion execution frequency
PID Controller Update Rate	100 Hz	Real-time motion stabilization
Average Localization Error	±7.2 cm	Pool trajectory evaluation
Heading Stabilization Error	±2.4°	During autonomous hovering
Mission Planner Tick Rate	20 Hz	BehaviorTree.CPP execution
DDS Packet Reliability	98.7%	After Cyclone DDS tuning
Autonomous Gate Detection Range	3-4 m	Under controlled pool lighting
Autonomous Mission Success Rate	84%	Across repeated pool trials
Recovery Behavior Response Time	<0.9 s	During simulated node failure
Simulation-to-Real Transfer Accuracy	~87%	Navigation behavior consistency

APPENDIX: D

Table XII: Electrical Testing Plan and Results

Category	Validation Items	Observation / Result
Power System	Stable power distribution, regulated 5 V/12 V/24 V rails, full-load operation	Initial voltage drop observed during rapid thruster acceleration; resolved by adding distributed bulk capacitance and improving grounding layout
Thruster and Kill System	Kill switch response, recovery behavior, ESC validation	Early MOSFET switching instability caused delayed shutdown under high load; gate biasing and protection circuitry were redesigned, resulting in reliable immediate shutdown
Sensors	IMU, Bar30, and camera validation	IMU vibration noise affected localization during initial pool tests; software filtering and mounting isolation improved sensor stability
Communication	ROS2 communication and telemetry stability	Packet loss occurred during high-bandwidth telemetry streaming; resolved through DDS configuration tuning and topic rate optimization
Telemetry	System monitoring and data visualization	Stable live monitoring achieved after calibration of voltage and current sensing modules
Actuation	Torpedo deployment and servo response	Initial servo jitter observed due to electrical noise; isolated power regulation eliminated inconsistent actuation
Safety System	Leak detection and emergency shutdown	Leak probes successfully triggered emergency response during controlled water ingress testing

Table XIII: Hardware Testing and Results

Test	Description	Observation / Result
Preliminary Leak Test	Vacuum and submerged enclosure testing	Minor leakage detected around an early penetrator design; sealing mechanism was redesigned before final deployment
Buoyancy and Balance Test	Buoyancy and center-of-mass validation	Initial pitch imbalance reduced hover stability; ballast distribution was adjusted to achieve stable hovering
Thruster Mounting Test	Structural validation under dynamic loading	Early vibration observed at high thrust; reinforcement brackets improved rigidity
Bench Test	Sequential subsystem validation prior to deployment	Identified intermittent ESC communication failure caused by loose connectors; connectors were replaced and secured
Pool Test	Validation of navigation, hover stability, and autonomy	Initial depth oscillation observed due to PID tuning; controller gains were refined for smoother stabilization
Endurance Test	Long-duration underwater operation	Thermal buildup detected inside enclosure during early endurance runs; improved internal airflow and power scheduling stabilized operating temperatures

Table XIV: Software Test Plans and Results

Component / Capability	**Validation Objective**	**Methodology**	**Timeline**	**Observation / Result**
Sensor Drivers	Validate ROS2 sensor integration	Driver and hardware testing	March 2026	Initial synchronization mismatch between sensors resolved through timestamp alignment
Localization and Control	Validate EKF localization and PID control	Simulation and pool testing	March–April 2026	Early localization drift observed during aggressive turns; EKF tuning improved stability
Vision System	Validate YOLOv11 perception and XFeat/FLANN matching	Simulation and underwater testing	April 2026	Detection accuracy decreased under low lighting; dataset augmentation improved robustness
Mission Planner	Validate autonomous task execution	Simulation and in-water trials	April–May 2026	Initial state transition failures occurred during interrupted missions; recovery logic was added
ROS2 Hybrid Architecture	Validate Humble–Jazzy communication	Cross-device testing	April 2026	DDS instability under heavy traffic resolved through Cyclone DDS tuning
Autonomous Navigation	Validate waypoint tracking and obstacle handling	Gazebo Harmonic and pool testing	May 2026	Navigation overshoot observed during sharp turns; controller parameters refined
Actuation System	Validate torpedo deployment	Manual and autonomous tests	May–June 2026	Inconsistent trigger timing observed initially; synchronization logic corrected
Full System Integration	Validate mission-level autonomy	Combined simulation and underwater testing	June 2026	Full autonomous mission sequence completed successfully after iterative subsystem refinements

APPENDIX: E
Table XV: COMPONENT LISTS

Component	**Vendor**	**Model / Type**	**Specifications**	**Custom / Purchased**	**Year**	**Cost**
Buoyancy Control	Blue Robotics	Buoyancy Foam R3318	6 pieces	Purchased	2025	$300
Frame	Local	Custom Aluminum, T-slot Aluminum Extrusion Bar	Custom design	Custom	2026	$50
Waterproof Housing	Local	Custom Aluminum Box Shape	Aluminum 6061 with rubber sealer	Custom	2026	$200
Waterproof Connectors	Blue Robotics	WetLink Penetrator	M10 - 6.5 mm - HC	Purchased	2025	$130
Frame Anodizing	Rainbow Gloss Black (39)	Black	Coating finish	Purchased	2026	$10
Thrusters	Blue Robotics	T200 Brushless Thruster	High thrust underwater motor	Purchased	2025	$1600
Motor Control	Blue Robotics	Basic ESC	3 Phase Electronic Speed Controllers	Purchased	2025	$320
Low-Level Control	Robotics Bangladesh	Raspberry Pi 5	64-bit quad-core Arm Cortex-A76 processor, 8GB Ram	Purchased	2026	$200
Actuators	Robotics Bangladesh	MG996R	180-degree servo motor	Purchased	2025	$14
Battery	EEE Tech	Li-ion 5S 18.5V 15000mAh	High density battery	Purchased	2026	$150
Converter	Robotics Bangladesh	Buck Converter	5-40V to 1.2-12V step-down	Purchased	2025	$10
High Level Control/CPU	Nvidia	Jetson Orin Nano	6-core CPU, 1024-core GPU, 20 TOPS	Purchased	2025	$600
Internal Comm Network	N/A	CAN, I2C	Communication protocols	N/A	2025	N/A

External Comm Interface	Blue Robotics	Fathom ROV Tether (ROV-ready)	High-speed data link	Purchased	2026	$440
Programming Language 1	N/A	C++	System programming	N/A	2025	N/A
Programming Language 2	N/A	Python	AI & scripting	N/A	2025	N/A
Compass and IMU	VectorNav	VN200	GPS-aided 9-axis high-precision IMU	Purchased	2025	$3500
Camera 1	Luxonis	OAK-D-W	12 MP RGB camera module with autofocus	Purchased	2025	$649
Camera 2	Intel	Intel RealSense Depth Camera D455	Stereo Depth 120 FPS Viewing Angle 90° × 65°	Purchased	2026	$620
Hydrophones	Aquarian Audio	H1a	4.5mm OD hydrophone	Purchased	2025	$366
Manipulator	BengalSub	Custom	ABS + TPU custom gripper	Custom	2025	$50
Algorithms: Vision	N/A	YOLO V11	Real-time object detection	N/A	2025	N/A
Algorithms: Acoustics	N/A	TDoA	Time Difference of Arrival	N/A	2025	N/A
Algorithms: Localization/Mapping	N/A	ROS2	Robot operating system stack	N/A	2026	N/A
Open Source Software	N/A	ROS, Gazebo	Simulation & robotics frameworks	Open Source	2025	N/A
Team Size	N/A	N/A	25 people	N/A	2026	N/A
HW/SW Expertise Ratio	N/A	N/A	1:3	N/A	2026	N/A
Testing Time: Simulation	N/A	N/A	280 hours	N/A	2026	N/A

APPENDIX: F
COMMUNITY OUTREACH


১৪ প্রজন্ম
সম্ভাবনা, উদ্যোগ ও সাফল্যের গল্প
ittefaq.youth@gmail.com

সোমবার
২৫ মে ২০২৬
১১ জ্যৈষ্ঠ ১৪৩৩

দৈনিক ইত্তেফাক

আন্ডারওয়াটার রোবটিক্সের বিশ্বমঞ্চে বাংলাদেশের তরুণরা

■ সৈয়দ তাওসিফ মোনাওয়ার

বিজ্ঞাপন তৈরিতে এআই ব্যবহার সোহান যেভাবে নজর কাড়ছেন

■ নওসাদ আল সাইম

নতুন প্রজন্মের জন্য বাংলাদেশের টেকসই স্থাপত্যচর্চা নিয়ে গবেষণা প্রতিবেদন

■ প্রজন্ম ডেস্ক

Crumb News
1d ·

From a successful debut in 2025 to a bold return in 2026, Team BengalSub is ready to dive deep on the world stage. Representing Bangladesh, this talented group of innovators is heading to California this July to compete in RoboSub 2026, the premier international Autonomous Underwater Vehicle (AUV) competition. After securing the 41st spot in their first outing, the team is now set to challenge global engineering giants like Cornell and Carnegie Mellon.

Led by Sudipto Mondal and supported by a diverse team of dedicated specialists, BengalSub is transforming complex robotics into reality. Their journey is more than a competition: it is a testament to the growing prowess of Bangladeshi tech talent. With grit and ingenuity, these young minds are proving that they belong among the world's best.

Fig. 25: STEM Engagement

Team BengalSub is deeply committed to inspiring the next generation of innovators through active STEM outreach. As part of our initiative, our team members conducted interactive sessions at local schools, where we introduced students to the fundamentals of robotics, underwater technology, and real-world engineering. A photograph of the community outreach and stem engagement is shown in **Fig. 25**. Through hands-on demonstrations, including showcasing our AUV components and control systems, we sparked curiosity and encouraged young minds to explore science and engineering. These sessions were designed to be engaging, inclusive, and practical allowing students to ask questions, interact with components, and understand how classroom knowledge translates into cutting-edge robotic applications. Our goal is to make STEM more accessible and exciting, especially for students in underserved communities, and empower them to dream big in the fields of technology and innovation.

APPENDIX: G
TOOLS & EQUIPMENTS

1) Electrical Equipment
   - Solder gun and stand
   - Solder wire
   - Wire strippers (standard and AWG precision)
   - Ethernet cables and LAN spool
   - HDMI cables
   - Micro USB cables for screens
   - Test screen
   - Multimeter
   - Spare, charged Li-Po batteries
   - Battery chargers (Li-Po compatible)
   - Extension cords and power strips
   - Screwdrivers (various sizes)
   - USB extenders and hubs
   - Scissors
   - USB ASP programmer
   - Glue gun and glue sticks
   - Arduino Uno boards with cables
   - Spare ATmega and CAN ICs
   - Duct tape and insulation tape
   - Jumper wires
   - Single-strand and AWG wires for harnessing
   - Mouse and keyboard
   - Heat shrinks tubing and heat gun
   - Crimping tools and connectors
   - XT60, XT30 connectors
   - Digital oscilloscope (for signal debugging)
   - Bench power supply
   - PDB test board
   - USB-to-UART interfaces
   - Hot air rework station (for PCB repairs)

2) Mechanical Equipment
   - Allen key and spanner set
   - Precision screwdrivers (PSD)
   - Drill machine with assorted bits
   - Epoxy resin, mixing cups, sticks
   - Cardboard, tissue, chalk for layout work
   - Duct tape, insulation tape
   - Zip ties (various sizes)
   - Rope for handling and lowering AUV
   - Nuts, bolts, washers (stainless steel preferred)
   - Buoyancy foam and floats
   - Mini hacksaw and blade replacements

- Scissors and utility knife
- Calipers and measuring tape
- Sandpaper for edge finishing
- Thread locker for critical fasteners
- Ballast weights and mounting straps

3) Testing and Integration Equipment

- Water tank or access to pool for testing
- Fathom ROV Tether and slip ring.
- Kill switch test harness
- Tether booster modules
- ROS2 Jazzy and Humble
- Jetson Orin Nano and Raspberry Pi 5 for integration testing
- Eclipse Cyclone DDS
- Arduino and ESP32 microcontroller
- Cameras (Intel Real Sense D455, low-light USB) for vision pipeline validation
- Spare thrusters and ESCs for quick swap during pool tests
- Digital scale for weight checks
- Leak detection sensors and vacuum pump for hull testing

Fig. 26: After a successful autonomous pool testing.